J. Fluid Mech. (1983), *vol.* 134, *pp.* 33–47
Printed in Great Britain

Noise generated by airfoil profiles placed in a uniform laminar flow

By H. ARBEY AND J. BATAILLE
Laboratoire de Mécanique des Fluides, associé au CNRS,
Ecole Centrale de Lyon, 69130 Ecully, France

(Received 15 January 1983)

The present paper is devoted to the experimental study of the noise generated by an airfoil profile placed in a uniform laminar flow. The far-field acoustic spectrum is shown to be composed of a broadband contribution around frequency f_s and a discrete contribution at equidistant frequencies f_n, which follow power laws of the forms $f_s \sim U^{1.5}$ and $f_n \sim U^{0.85}$. Both contributions can be accounted for by a simple model derived from the original suggestions of Tam (1974) and Fink (1975). It is essentially assumed that the diffraction of the Tollmien–Schlichting instabilities by the trailing edge generates acoustic waves which propagate in the far field and also trigger an aeroacoustic feedback loop, whose length is equal to the distance between the trailing edge and the maximum velocity point of the airfoil.

1. Introduction

In recent years, a few papers (Paterson *et al.* 1972; Sunyach *et al.* 1973; Tam 1974; Fink 1975; Schlinker, Fink & Amiet 1976; Fathy, Rashed & Lumsdaine 1977) have been devoted to the study of discrete frequencies emitted by airfoils placed in a laminar flow whose Reynolds number, based on the chord, did not exceed some critical value of the order of 6×10^5, associated with boundary-layer transition. The most significant of the above contributions is that of Paterson, who showed that the Strouhal frequency f of the observed narrowband spectrum exhibited a so-called 'ladder-type' variation, i.e. was a piecewise continuous function of the flow velocity U which increased locally according to an $f \sim U^{0.8}$ power law and underwent a number of jumps (figure 1). In some cases, however, two distinct frequencies were observed for the same value of the velocity (see points A and B on figure 1). Moreover, the average evolution of the frequency – smoothing out all jumps – proved to follow an $f \sim U^{1.5}$ law. Finally, Paterson found that this phenomenon only occurred when the boundary layers developing on the airfoil were laminar, at least on the pressure side, and that the trailing edge played a crucial role in the sound-generation process. In order to explain the behaviour described above, three different models, namely the vortex model, the aeroacoustic feedback model, and the unstable boundary-layer model, were suggested by various authors. In the vortex model, Paterson *et al.* (1972) made the very questionable assumption that a vortex region developed from the trailing edge of the airfoil as it would downstream of a blunt body, implying the constancy of a Strouhal number $f(2\delta)/U$, based on the width of the wake, taken here to be twice the thickness δ of the boundary-layer at the trailing edge. As a consequence, the average law $f \sim U^{1.5}$ was recovered, although the authors were unable to explain the ladder-type structure. According to Tam's feedback model, the instabilities of the boundary layer, as they grow and propagate downstream, induce

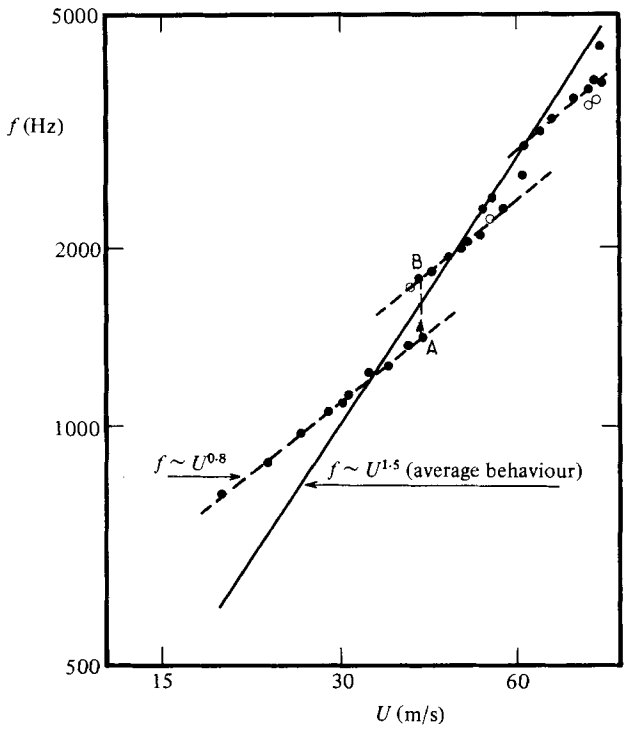

FIGURE 1. Ladder-type structure of the dominant frequency with flow velocity (from Paterson *et al.* 1972).

a strong-enough lateral vibration in some highly localized region of the wake, which acts as a noise source. The acoustic waves it emits in the upstream direction in turn enhance the oscillation of the boundary layer. The phase condition necessary for the existence of such a self-excited feedback loop is consistent with the existence of several distinct frequencies at a given velocity. Tam's argument, however attractive it is, is unfortunately merely qualitative and does not account for the $U^{1.5}$ average law or for the frequency jumps. In Fink's model the boundary-layer disturbances, which are convected downstream, are postulated to radiate noise as they are diffracted by the trailing edge of the airfoil. The $U^{1.5}$ average law for the Strouhal frequency is derived from classical hydrodynamic-stability theory. But the physical argument used by Fink to explain the other characteristics of the noise spectrum is neither convincing nor supported by experiment.

Although it is recognized here that both Tam's and Fink's models are consistent with part of the special features of the experiment, none of the various theories proposed so far is entirely satisfactory. It is quite clear that a better understanding of the role played by the instability of the boundary layer is needed. In order to identify and separate the different mechanisms involved, new experiments were carried out. In §2 the facility and the experimental conditions are described in detail. In §3 the spectrum of the radiated noise is shown to consist of a broadband contribution whose dominant frequency is f_s, and a sequence of discrete frequencies denoted by f_n. Moreover, the ladder-type evolution of the peak frequency proves to be an obvious consequence of the empirical laws obtained for the variation with the flow velocity of f_s ($\sim U^{1.5}$) and f_n ($\sim U^{0.85}$). Section 4 is devoted to the physical

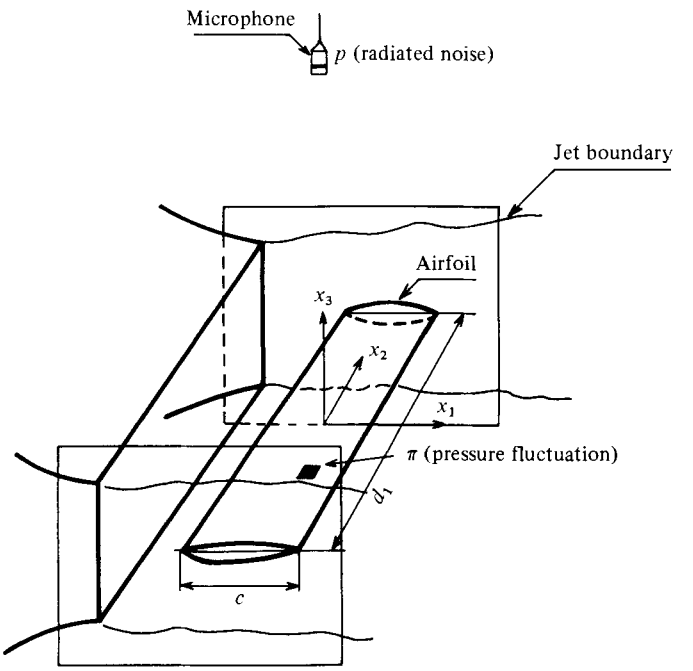

FIGURE 2. Experimental set-up.

understanding of the mechanisms involved in the above findings. It is shown that the broadband contribution is associated with the diffraction of the Tollmien–Schlichting waves by the trailing edge and that the resulting acoustic waves trigger an aeroacoustic feedback loop which generates the discrete frequencies f_n. Such a model proves to be consistent with the experimental data.

2. Experimental conditions

The airfoil, placed at 0° incidence, was located 10 cm downstream of the outlet section (15 cm × 30 cm) of a convergent nozzle of contraction ratio 2 (see figure 2). Three different aerofoils were selected in order to study separately the influence of the Reynolds number ($Re = Uc/\nu$) at constant velocity and external pressure gradient (NACA 0012.8 and NACA 0012.16) and that of the external pressure gradient at constant velocity and Reynolds number (NACA 0012.16 and NACA* 0012.16). The last number in the specification of the profile refers to the chord length expressed in centimetres. The NACA* 0012.16 profile is derived from the original NACA 0012.8, as shown in figure 3(*a*). The corresponding potential-velocity distributions, which were calculated using Henry's (1975) method of singularities, are quite different (see figure 3*b*). The far-field noise was measured by a 1 in. Bruel & Kjaer microphone located at 1.9 m from the airfoil on the normal to its chord. The characteristics of the pressure field induced by the boundary layer in the vicinity of the trailing edge were provided by 1.5 mm chordwise pressure transducers whose detailed description is available in Arbey (1981). In what follows, we shall essentially rely on the data provided by the transducer located near the trailing edge ($x/c = 0.88$). The characteristics of the boundary layer which proved necessary when interpreting our results were both calculated (Mari, Jeandel & Mathieu, 1976) and

x_1/c	0	0.0125	0.025	0.05	0.075	0.10	0.15	0.20
x_3/c	0	0.0131	0.0178	0.0234	0.0267	0.0287	0.030	0.030
x_1/c	0.65	0.70	0.75	0.80	0.90	0.95	0.975	1
x_3/c	0.030	0.029	0.0265	0.0228	0.0131	0.0073	0.0041	0.0007

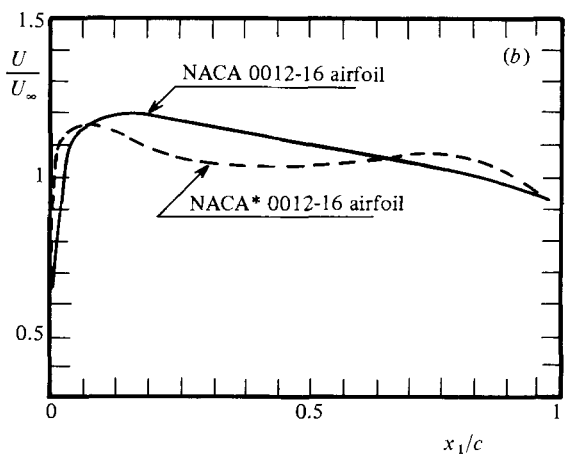

FIGURE 3. (*a*) Characteristics of the NACA* 0012.16 airfoil. (*b*) Potential velocity distributions for the airfoils.

determined experimentally from mean-velocity profiles near the trailing edge and from visualizations of the flow. The reader is referred to Arbey (1981) for additional information. The spectra were measured using a NICOLET 660A analyser, whose bandwidth was less than 1 Hz.

3. Experimental results

3.1. *Existence of two contributions*

Typical spectra of the noise radiated in the far field by the airfoils for a great number of values of the flow velocity within the range 20–42 m/s are shown in figures 4(*a–c*). Broadly speaking, they exhibit a peak which is reminiscent of the Strouhal frequency first found by Paterson. A very careful inspection of the signal which was made possible by the high resolution of the analyser revealed, however, that this peak results in fact from the superposition of a broadband contribution around a frequency f_S and a set of regularly spaced discrete frequencies f_n. As many as twelve were observed in the range 1000–2500 Hz, with a constant spacing Δf of the order of

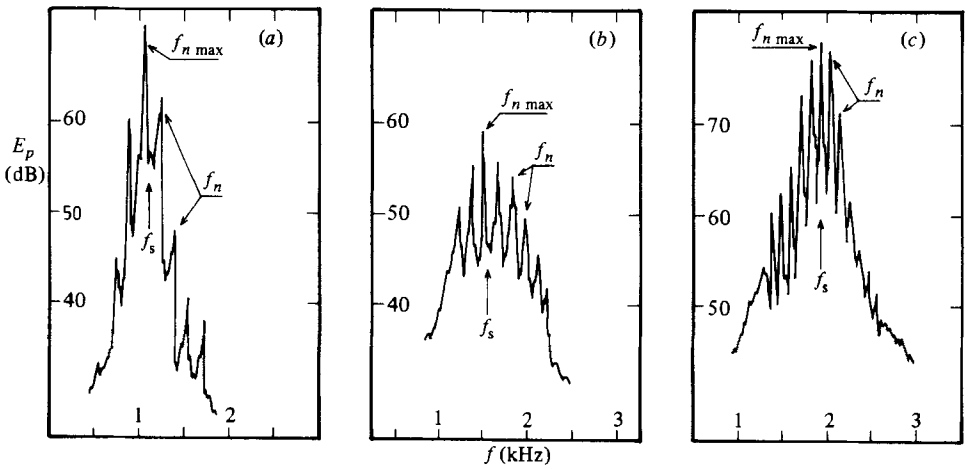

FIGURE 4. Typical radiated noise spectra: (*a*) NACA 0012.8, $U = 20.2$ m/s; (*b*) NACA 0012.16, $U = 35$ m/s; (*c*) NACA* 0012.16, $U = 35$ m/s.

110 Hz. That frequency which coincides with f_s – hereinafter denoted by $f_{n\,\max}$ – obviously plays a special role since it corresponds to the peak of the spectrum. Similar observations were made concerning the spectrum E_π of the pressure fluctuations at the wall close to the trailing edge. The variation of the above-defined frequencies – i.e. f_s, f_n and $f_{n\,\max}$ – with the flow velocity is analysed in detail in §§3.2–3.4.

3.2. *Behaviour of the peak frequency f_s of the broadband contribution*

Rather than f_s itself, it proved convenient when interpreting the experimental data (see §4.1) to consider the Strouhal number

$$St_s = \frac{f_s \delta_1}{U} \tag{1}$$

based on the displacement thickness δ_1 of the boundary layer at the trailing edge. This number was determined for each run from the measured values of f_s and the numerically computed values of δ_1 (Mari *et al.* 1976) given in table 1. It is observed (figure 5) that, whatever the airfoil investigated, all the experimental points lie, to within better than 15%, on the horizontal line defined by

$$St_s = 0.048 \pm 0.003 \quad \forall Re. \tag{2}$$

The corresponding empirical relation for f_s turns out to coincide with Paterson's $U^{1.5}$ average law

$$f_s = 0.011 U^{1.5} (c\nu)^{-\frac{1}{2}}. \tag{3}$$

Although this result is not unexpected, it deserves a discussion (see §3.4), since Paterson's equation (3) refers to a mean fictitious behaviour of the dominant frequency F of the overall spectrum E_p, whereas here f_s denotes the peak frequency of the broadband contribution to E_p.

3.3. *Behaviour of the discrete frequencies f_n*

In table 2 the value of the difference Δf between two consecutive discrete frequencies f_n is given along with the numerically determined distance L (Henry 1975) between the maximum velocity point and the trailing edge of the airfoil. Whatever the profile

NACA 0012.16; $i = 0°$			NACA* 0012.16; $i = 0°$			NACA 0012.16; $i = 0°$		
U (m/s)	f_s (Hz)	δ_1 (mm) calculated from Mari	U (m/s)	f_s (Hz)	δ_1 (mm) calculated from Mari	U (m/s)	f_s (Hz)	δ_1 (mm) calculated from Mari
21.02	769	1.338	20.24	925	1.123	20.2	1149	0.90
22	835	1.308	21.02	1029	1.102	30.4	1990	0.73
24.93	1026	1.229	23.76	1244	1.036			
26.79	1140	1.185	25.60	1331	0.998			
29.11	1259	1.137	27.61	1414	0.961			
30.47	1307	1.111	28.89	1480	0.940			
31.88	1432	1.087	31.4	1697	0.901			
32.99	1498	1.068	32.74	1789	0.883			
34.66	1592	1.042	34.26	1872	0.863			
35.99	1717	1.023	36.13	2129	0.840			
37.95	1852	0.996	38.53	2297	0.814			
39.12	1895	0.981	40.63	2459	0.792			

TABLE 1. Peak frequency of the broadband contribution and displacement boundary-layer thickness at the trailing edge for various profiles and different flow conditions

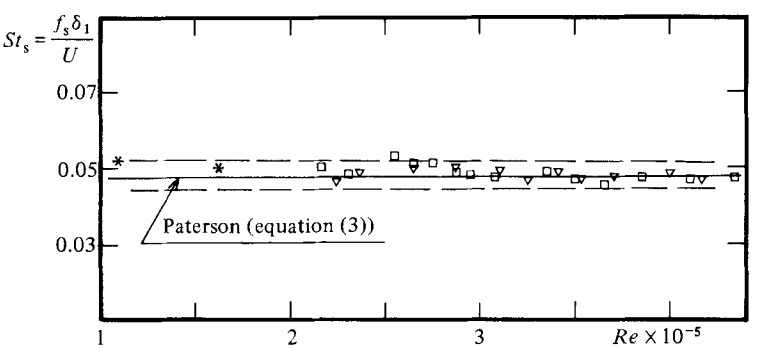

FIGURE 5. Effect of Reynolds number Re on the Strouhal number St_s deduced from the main frequency f_s of the measured broadband spectrum: *, NACA 0012.8; ▽, NACA 0012.16; □, NACA* 0012.16.

investigated here (NACA 0012.8, NACA 0012.16, NACA* 0012.16) and the flow velocity within the interval 20–42 m/s, Δf was inversely proportional to L. In fact, the result holds for a much larger range of velocities (20–120 m/s), and even at non-zero incidence ($0° \leqslant i \leqslant 10°$), since the same conclusion was drawn from Paterson's data, which concern various NACA profiles at incidence and higher Reynolds numbers. More precisely, the behaviour of Δf is given by the following empirical law (figure 6):

$$L\Delta f = KU^m, \tag{4}$$

where $K = 0.89 \pm 0.05$, in m.k.s. units and $m = 0.85 \pm 0.01$, or preferably by

$$\frac{L\Delta f}{U} = 0.37 M^{-0.15}. \tag{5}$$

It should be noted, however, that this dimensionless correlation only involves variations of the Mach number of the flow M associated with variations of U, since the velocity of sound a_0 was constant in the above-mentioned experiments.

	Present results							Paterson's data									
Profile ...	NACA 0012.16			NACA* 0012.16			NACA 0012.8	NACA 0018.23		NACA 0012.23							
i ...	0°			0°			0°	10°		4°			6°			10°	
L (m) ...	0.138			0.150			0.069	0.1436		0.194			0.156			0.078	
U (m/s) ...	22.02	31.94	40.58	20.2	31.55	40.71	20.2	33.21	41.84	30.5	39.66	46.70	19.19	31.64	42.39	37.96	43.87
Δf (Hz) ...	98	129	159.5	69	102	127	166	126	146	—	109	120	—	—	149	—	279
f_n (Hz)																	
$n = 4$	—	—	—	—	—	—	747	—	—	—	—	—	—	—	—	1129	1288
5	510	—	—	—	—	—	913	—	—	—	—	—	—	—	—	—	1579
6	610	—	—	—	—	—	1079	—	—	—	—	—	—	—	—	—	1846
7	715	—	—	532	—	—	1245	—	—	—	—	—	—	—	—		
8	806	1112	1355	600	—	—	1411	—	—	—	—	—	—	—	—		
9	901	1243	1524	669	—	—	1577	1127	—	—	—	—	—	—	—		
10	1000	1363	1671	737	—	—	1743	—	—	—	—	—	740	1121	1422		
11	1095	1494	1835	811	—	—	—	—	1692	—	—	—	—	—	—		
12	1194	1636	2005	883	1293	1593	—	1507	1809	—	—	—	—	—	1720		
13	1291	1767	2157	951	1391	1721	—	—	1954	1109	1388	—					
14	—	1887	2313	1017	1494	1849	—	—	—	—	—	1706					
15	—	2015	2470	1088	1592	1977	—	—	—	—	—	—					
16	—	—	2631	—	1700	2111	—	—	—	—	1710	—					
17	—	—	—	—	1803	2239	—	—	—	—	—	—					
18	—	—	—	—	1901	2361	—	—	—	—	—	—					
19	—	—	—	—	1999	2495	—	—	—	—	—	2304					
20	—	—	—	—	2107	2610											
21	—	—	—	—	2215	2741											
22	—	—	—	—	2318	2872											
23	—	—	—	—	2416	2994											

TABLE 2. Discrete frequencies f_n for various profiles and different flow conditions (L calculated from Henry)

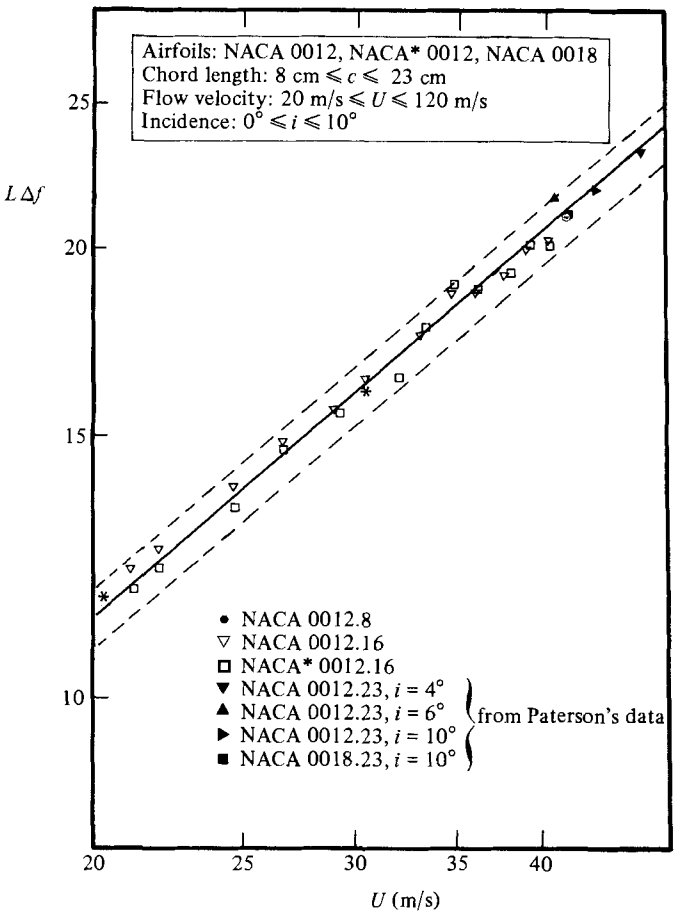

FIGURE 6. Effect of flow velocity U on the value of $L\Delta f$.

Moreover, the Strouhal number defined by

$$St_n = \frac{f_n L}{u^*}$$

(where, according to (4) $u^* = KU^m$) proved to remain constant under all experimental conditions investigated by Paterson and the authors (see figure 7) with

$$St_n = \frac{f_n L}{u^*} = (n+\tfrac{1}{2}) \pm 0.02. \tag{6}$$

The associated empirical law for f_n is therefore

$$f_n = (n+\tfrac{1}{2})\frac{K}{L} U^{0.85}. \tag{7}$$

3.4. *Ladder-type variation of* $f_{n\max}$

The dominant discrete frequency $f_{n\max}$ is a discontinuous function of the flow velocity, as shown in figure 8(*a*) for the NACA 0012.16 profile, while f_s and f_n have a smooth variation. This 'ladder-type' behaviour, which was mentioned for the first time by Paterson, can now be easily explained. Indeed, if the value of the flow

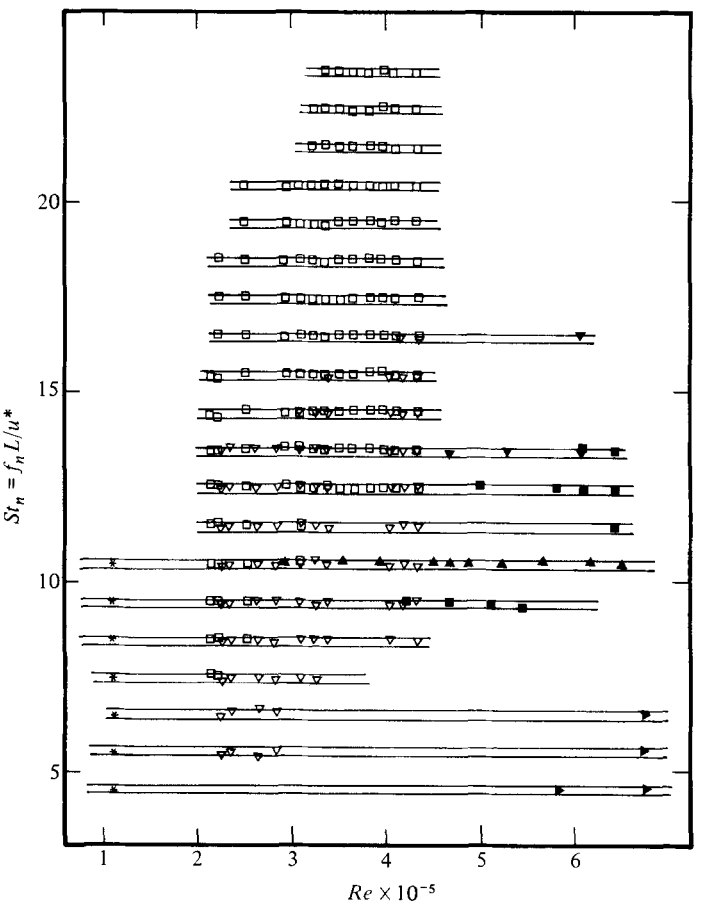

FIGURE 7. Effect of Reynolds number Re on the Strouhal number St_n associated with the discrete frequencies of the radiated noise spectrum (same aerodynamic conditions as figure 6).

velocity, say U_1, is such that f_n is equal to f_s, their common value is the dominant frequency of the overall noise spectrum (figure 8*b*). When the velocity of the flow grows, f_s practically increases by twice as much as f_n, according to (3) and (7). Eventually, for some velocity U_2, two discrete frequencies corresponding to the same amplitude will appear. If the flow velocity keeps increasing, it will reach a value U_3, for which f_s coincides with f_{n+1}, and so on .... Moreover, it is clear that the dominant frequency F observed by Paterson should indeed be identified with f_s (see figure 5) since the broadband contribution, on which the discrete spectrum is superimposed, imposes the value of the dominant frequency of the overall noise spectrum.

A full justification of the phenomena reported in this paragraph requires a clear understanding of the physical mechanisms that are responsible for the power-law behaviour of f_s (equation (3)) and f_n (equation (7)) and for the coexistence of several discrete frequencies at a given velocity.

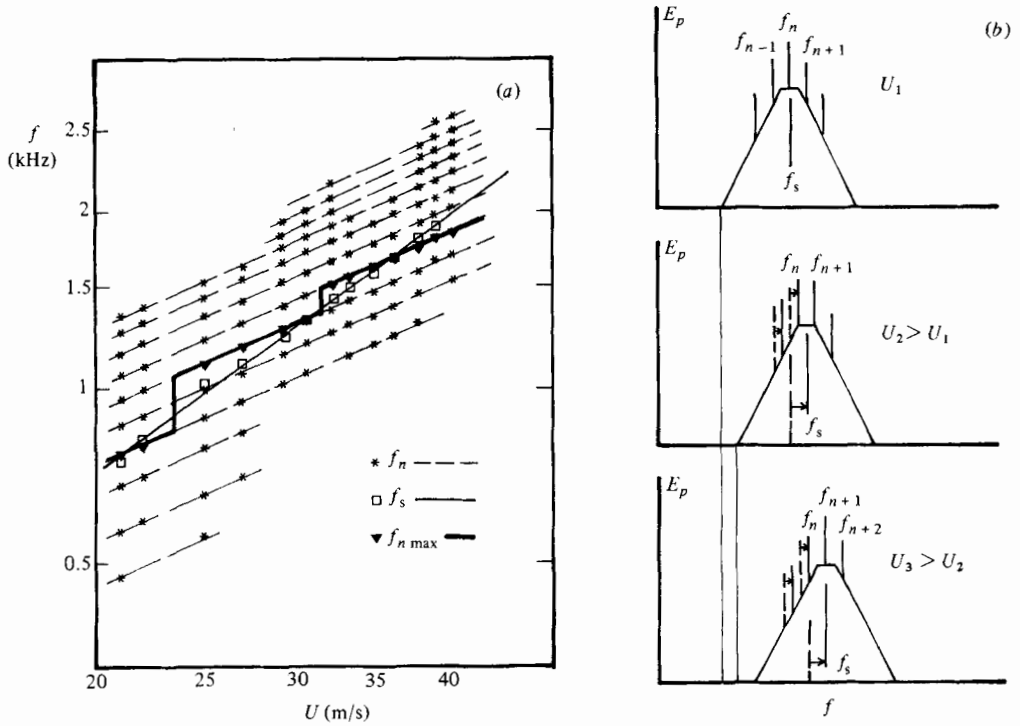

FIGURE 8. Ladder-type evolution of the dominant discrete frequency $f_{n\,max}$ with flow velocity (NACA 0012.16 airfoil).

4. Physical interpretation

4.1. *Broadband contribution*

The great similarity between the far-field acoustic spectrum E_p and the wall-pressure spectrum near the trailing edge E_π, which exhibit the same peak f_s (figure 9), along with the constancy of the Strouhal number St_s (figure 5), confirm Fink's (1975) assumption that the broadband contribution to the radiated noise results from the diffraction, by the trailing edge, of the hydrodynamic fluctuations induced by the instability of the boundary layer. The mechanism proposed by Ffowcs Williams & Hall (1970) and also by Howe (1978) to explain such an emission, when turbulent boundary layers are concerned, can reasonably be extended here, although the boundary layer is transitional, because the fluctuating pressure fields at the wall are analogous in both cases. Besides, the amplitude of the pressure fluctuation close to the trailing edge ($\pi'/\frac{1}{2}\rho U^2 = 0.14$) measured by Arbey (1981), which is roughly the same as that observed by Archibald (1975) ($\pi'/\frac{1}{2}\rho U^2 = 0.17$) in a transitional boundary layer, is much greater than the value expected for a turbulent boundary layer ($\pi'/\frac{1}{2}\rho U^2 = 0.007$).

Linear stability theory of boundary layers predicts rather well the shape of the wall-pressure spectrum (see figure 9) as was shown by Arbey (1981). Such an approach, however, is not accurate enough when the variation of f_s with U is to be determined. Instead, use was made of the fact that at any point of the airfoil, and for a given Reynolds number, the frequency f_s – which is that of the hydrodynamic perturbation of maximum amplitude – is the same as the frequency given by the

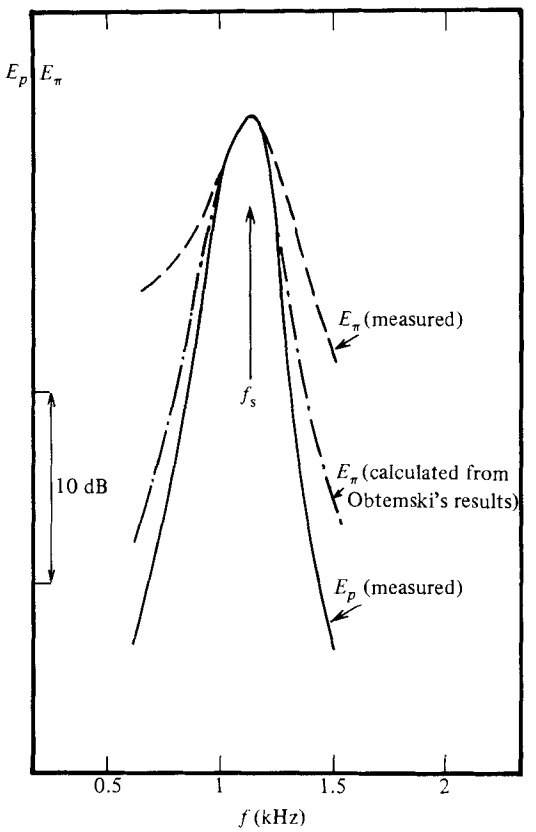

FIGURE 9. Comparison between the broadband components of spectra E_p and E_π (NACA 0012.8, $U = 20$ m/s).

upper neutral stability curve obtained by Obremski *et al.* (1969). It is important to note that this statement, which was first made by Fink (1975) in the absence of any external pressure gradient, in fact only holds for adverse external pressure gradients (Arbey 1981), as is the case here. From the curves of Obremski *et al.* it is straightforward to show (see figure 10) that the Strouhal number is, whatever the Reynolds number, a constant given by

$$St_s = \frac{f_s \delta_1}{U} = 0.048. \tag{8}$$

The latter result is consistent with Paterson's correlation – equation (3) – derived from dimensional analysis.

4.2. *Discrete components*

The existence of a set of regularly spaced discrete frequencies f_n (figure 7) strongly suggests that an aeroacoustic feedback mechanism, analogous to that described by Wright (1976) and Longhouse (1977), and also by Tam (1974), takes place inside the unstable boundary layer. Specifically, it is assumed that the hydrodynamic fluctuations, which are convected at a velocity c_r inside the boundary layer, generate, as they are diffracted by the trailing edge, acoustic waves which propagate upstream and reach point A (see figure 11), where the hydrodynamic instabilities are created.

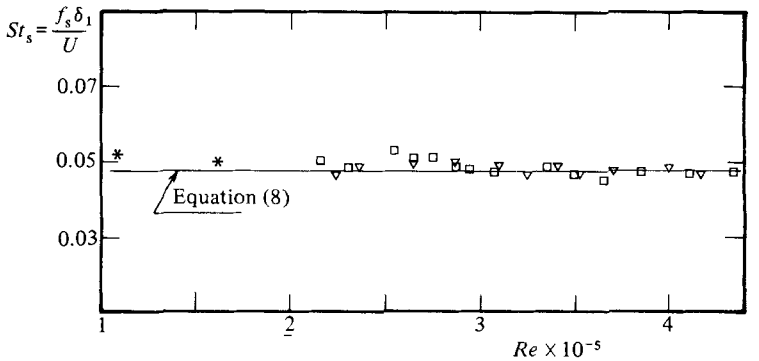

FIGURE 10. Behaviour of St_s: *, NACA 0012.8; ▽, NACA 0012.16; □, NACA* 0012.16.

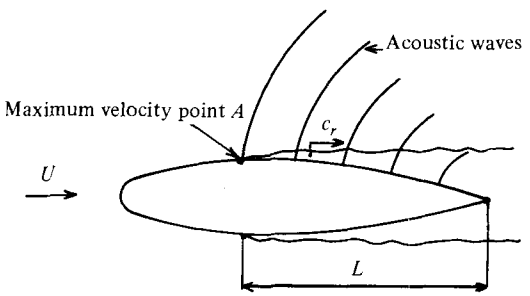

FIGURE 11. Aeroacoustic feedback loop.

If both the acoustic and the hydrodynamic signal are in phase at this point (Tam 1974; Archibald 1975) it is expected that the latter will undergo an amplification. It is believed here that point A is the maximum velocity point on the airfoil. That this should be the case is consistent with the fact that upstream of A the pressure gradient is favourable and the flow is stable, since the local Reynolds number is subcritical, while downstream of A instabilities develop owing to the adverse pressure gradient. This assumption is suggested by Archibald's findings concerning the behaviour of unstable boundary layers excited by acoustic waves. It is confirmed both by our experiments and those of Paterson *et al.* (1972). Indeed, in the present investigation (see figures 4*b*, *c*), for given values of the velocity and the chord ($U = 35$ m/s, $c = 16$ cm), the spacing between discrete frequencies depends on the particular profile used, NACA 0012.16 or NACA* 0012.16, which essentially differ by the position of the maximum velocity point. In Paterson's experiments, however, the latter point changed as a result of the modification of the incidence of the profile (see table 2). causing a significant variation of the distance L from 19.4 cm at $i = 4°$ to 7.8 cm at $i = 10°$.

As regards the dominant role played by the trailing edge in the generation of discrete tones, the reader is referred to the experiments of Paterson *et al.* (1972) and of Sunyach *et al.* (1973), who detected the presence of acoustic waves travelling upstream from it inside the boundary layer; and also to the work reported by Arbey (1981) and Gaudriot *et al.* (1982), who confirmed that the source of such sounds was to be found close to the trailing edge, using an acoustic imaging technique.

In view of Yu & Tam's (1977) conclusions concerning turbulent boundary layers, the diffraction occurring at the trailing edge is associated with a 180° phase shift of

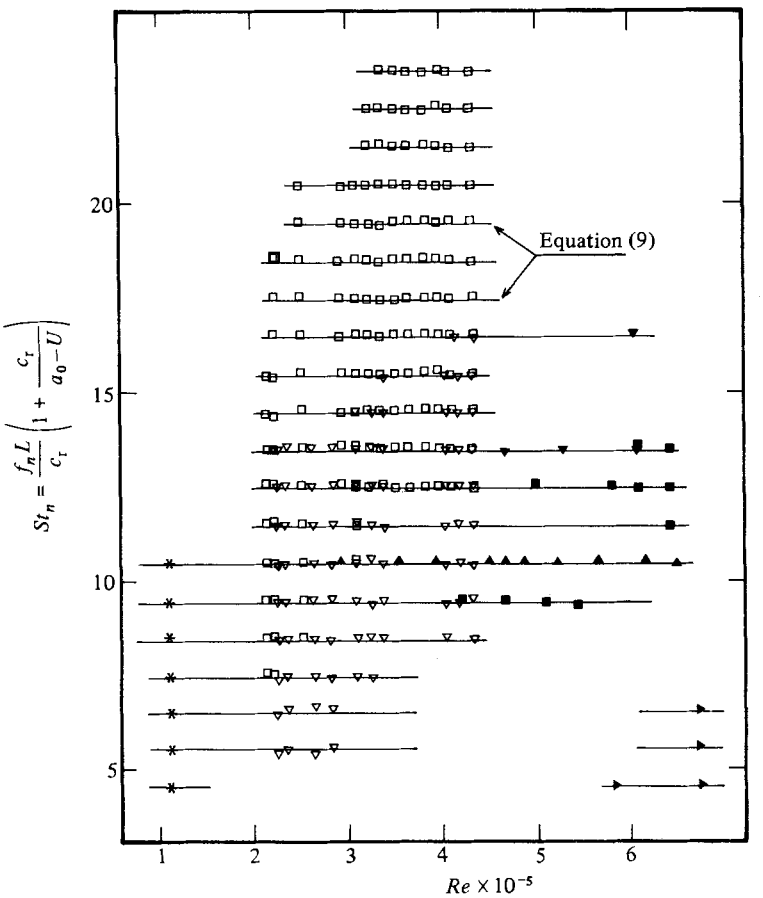

FIGURE 12. Behaviour of the Strouhal number St_n associated with the various discrete frequencies f_n. Present results: *, NACA 0012.8; ▽, NACA 0012.16; □, NACA* 0012.16. Paterson's results: ▼, NACA 0012.23, $i = 4°$; ▲, NACA 0012.23, $i = 6°$; ▶, NACA 0012.23, $i = 10°$; ■, NACA 0018.23, $i = 10°$.

the fluctuations. Accordingly, the following modified version of Tam's phase loop condition is proposed:

$$\frac{f_n L}{c_r}\left(1 + \frac{c_r}{a_0 - U}\right) = n + \tfrac{1}{2}. \tag{9}$$

All quantities appearing in this equation can be estimated for all profiles and Reynolds numbers, including c_r, which was calculated for each measured value of f_n using the numerical results of Obremski *et al.* Figure 12 shows that our data are in excellent agreement with the above model. In addition the velocity u^*, introduced as a convenience in §3.3, proves to be given by

$$u^* = \frac{c_r}{1 + c_r/(a_0 - U)}$$

if (6) and (9) are compared.

5. Conclusion

The use of appropriate aerofoil profiles placed in a uniform flow, along with a careful spectral analysis, made it possible to confirm and extend Paterson's findings concerning the generation of acoustic waves at discrete frequencies. The overall spectrum of the radiated noise proved to be composed of a broadband contribution with a peak at frequency f_s and of a set of equidistant discrete frequencies f_n, proportional respectively to $U^{1.5}$ and $U^{0.85}$, which explains the ladder-type evolution first brought out by Paterson. The broadband contribution was attributed to the diffraction of the instabilities developing in the boundary layer by the trailing edge of the airfoil, and its spectrum was shown to peak at a frequency f_s whose value, as calculated from the linear stability theory of laminar boundary layers, was in good agreement with experimental data. On the other hand it was established that the experimentally observed discrete frequencies could be recovered with an excellent approximation, using a modified version of Tam's aeroacoustic feedback loop whose length was equal to the distance between the trailing edge of the airfoil and its maximum velocity point.

One of the authors (H.A.) wishes to express his deep appreciation to Professor G. Comte-Bellot for her support and interest in the present work. Also fruitful discussions with Professor J. E. Ffowcs Williams are gratefully acknowledged.

REFERENCES

ARBEY, H. 1981 Contribution à l'étude des mécanismes de l'émission sonore de profils aérodynamiques placés dans des écoulements sains ou perturbés. Thèse de Doctorat ès Sciences, Université Claude Bernard, Lyon I.

ARCHIBALD, F. S. 1975 The laminar boundary layer instability excitation of an acoustic resonance. *J. Sound Vib.* **38**, 387–402.

FATHY, A., RASHED, M. I. & LUMSDAINE, E. 1977 A theoretical investigation of laminar wakes behind airfoils and the resulting noise pattern. *J. Sound Vib.* **50**, 133–144.

FFOWCS WILLIAMS, J. E. & HALL, L. H. 1970 Aerodynamic sound generation by turbulent flow in the vicinity of a scattering half plane. *J. Fluid Mech.* **40**, 657–670.

FINK, M. R. 1975 Prediction of airfoil tone frequencies. *J. Aircraft* **12**, 118–120.

GAUDRIOT, L., HELLION, A., BEGUET, B. & ARBEY, H. 1982 Analyse du bruit de profil par réseaux de capteurs proches ou lointains. *Rev. d'Acoust.* **63**, 208–210.

HENRY, C. 1975 Solution numérique par une méthode de singularités du problème de l'écoulement compressible sur des surfaces de courant axi-symétriques. Thèse de Docteur Ingénieur, Université Claude Bernard, Lyon I.

HOWE, M. S. 1978 A review of the theory of trailing edge noise. *J. Sound Vib.* **61**, 437–465.

LONGHOUSE, R. E. 1977 Vortex shedding noise of low tip speed, axial flow fans. *J. Sound Vib.* **53**, 25–46.

MARI, C., JEANDEL, D. & MATHIEU, J. 1976 Méthode de calcul de couche limite turbulente compressible avec transfert de chaleur. *Intl J. Heat Mass Transfer* **19**, 893–899.

OBREMSKI, H. J., MORKOVIN, M. V., LANDAHL, M., WAZZAN, A. R., OKAMURA, T. T. & SMITH, A. M. O. 1969 A portfolio of stability characteristics of incompressible boundary layers. *AGARDograph* 134.

PATERSON, R. W., VOGT, P. G., FINK, M. R. & MUNCH, C. L. 1972 Vortex noise of isolated airfoils. *AIAA Paper* 72–656.

SCHLINKER, R. H., FINK, M. R. & AMIET, R. K. 1976 Vortex noise from non rotating cylinders and airfoils. *AIAA Paper* 76–81.

SUNYACH, M., ARBEY, H., ROBERT, D., BATAILLE, J. & COMTE-BELLOT, G. 1973 Correlations between far-field acoustic pressure and flow characteristics for a single airfoil. *AGARD Conf.* **131**, *Noise Mechanisms*, Paper 5.

TAM, C. K. W. 1974 Discrete tones of isolated airfoils. *J. Acoust. Soc. Am.* **55**, 1173–1177.

WRIGHT, S. E. 1976 The acoustic spectrum of axial flow machines. *J. Sound Vib.* **45**, 165–223.

YU, J. C. & TAM, C. K. W. 1977 Experimental investigation of the trailing edge noise mechanism. *AIAA J.* **16**, 1046–1052.